Solar-light Driven Degradation of Methylene Blue by Titanium Oxide Nanoparticles (TiO_2 NPs)

Dikpal Kumar Shahi[1], Shukra Raj Regmi[1*], Narendra Prakash Shawad[1], Nurul Hoda Khan[1], Padam Raj Joshi[1], Lekha Nath Khatiwada[2], Rameshwar Adhikari[3]

[1]Central Department of Biological and Chemical Sciences, Mid-West University, Surkhet, Nepal

[2]Department of Customs, Ministry of Finance, Kathmandu Nepal

[3]Research Centre for Applied Science and Technology (RECAST), Tribhuwan University, Nepal

**Correspondance: shukra.regmi@mu.edu.np; Ph. 9849024059*

Keywords
Photocatalyst
TiO_2 NPs
Solar light degradation
Methylene blue

Received: 2 November 2024
Revised: 3 December 2024
Accepted: 13 December 2024

ISSN: 3059 - 9687

Abstract

Methylene blue is a common laboratory and textile dye that shows toxicity and carcinogenic activity in human health. In the present work, we have synthesized titanium oxide nanoparticles by the co-precipitation method through a controlled pH pathway for the degradation of methylene blue. The synthesized TiO_2 NPs are characterized by UV Spectrophotometer, Fourier Transfer Infrared (FT-IR), Electron Dispersive X-ray (EDX), and X-RD Crystallography. The average diameter of the particle 16.27 ± 12.80 nm is obtained by solving Debye Scherer's equation with crystallinity 57.15%. The photocatalytic degradation is carried out at the solar intensity of 5.76 ± 0.14 kWh and methylene blue degradation is recorded at 665 nm in UV-visible spectrophotometer. The result reveals that methylene blue is completely degraded in solar light within 110 minutes with 98% catalytic efficiency, but the dark medium degradation is not completed until 140 minutes and is limited to its 48% efficiency. The temperature-enhancing degradation in solar light is completed in 70 minutes with 98% efficiency. The catalytic efficiency of TiO_2 NPs in light is superior to that in the dark, which explores its potential application as a photocatalyst.

Introduction

Nanoparticles are unique due to their high surface atoms and variable particle size below 100 nanometers. Tuning of particle size affects the different chemical properties like adsorption, catalytic degradation, electronic properties, and optical phenomena. So, we can use these particles to increase efficiency in different fields like synthesis, medicine, energy, manufacturing industry, and electronic devices (Jamkhande *et al.*, 2019). Synthesis of Titanium Oxide nanoparticles is mostly carried out by bottom-up or top-down approach. Recently, green synthesis of Titanium Oxide nanoparticles (TiO_2 NPs) has also been reported with very low synthetic yield. Among them, chemical precipitation/co-precipitation, sol-gel method, chemical reduction method, and physical vapor deposition method are in application for low-cost synthesis. Similarly, laser ablation, molecular beam epitaxy, spray conversion processing, and self-assembly methods are implemented to synthesize different sizes and geometrical nanoparticles (Nyamukamba *et al.*, 2018; Rane *et al.*, 2018).

The TiO_2 nanoparticle exists in different geometrical forms like analase, rutile, and

brookite, which are very stable, non-toxic, and biocompatible. The nanocompounds of TiO_2 are considered one of the suitable photocatalysts due to their prominent optoelectronic properties. Among them, anatase is found to be a strong photocatalyst for the degradation of different dyes. The calculated band gap of TiO_2 is found to be 3.2 eV (Valencia *et al.*, 2010), which shows a strong effect of photocatalytic degradation of organic, inorganic, metallo-organic, and pesticides (Rane *et al.*, 2018). However, the catalytic efficiency of only TiO_2 NPs is low due to the fastest recombination of electron-hole pairs in TiO_2 NPs (Kumar *et al.*, 2022). The report shows that among the different synthetic pathways for TiO_2 NPs, the low temperature-controlled sol-gel method gives high purity and catalytic action (Akpan & Hameed, 2009). Photocatalytic degradation of dyes depends upon the pH, precursor concentration, catalytic purity, size, and intensity of light (Reza *et al.*, 2017). Thermally decomposed titanium tetra isopropoxide at around 700-1300 ^oC gives TiO_2 NPs, which is more effective for the photocatalytic degradation of methylene blue than the commercial catalyst (Chin *et al.*, 2010).

Photocatalytic decomposition of paracetamol by TiO_2 NPs in the presence of light at optimum pH 9.0. Their finding suggests that TiO_2/suspension is more efficient than TiO_2/fiber-based UV-photocatalytic degradation (Jallouli *et al.*, 2017). The catalytic degradation increases by removing organic carbon and dissolved nitrogen, accelerating the efficiency by 16% to 42% for p-nitrophenol (Shaoqing *et al.*, 2010). The photocatalytic degradation of Erichrome black T by titania shows that about 82% degradation was carried out in 50 minutes, which obeys pseudo-first-order kinetics with superior degradation properties (Kansal *et al.*, 2013). Malakotium M., *et al.*, 2020 reported that photocatalytic degradation of ciprofloxacin by TiO_2 NPs found effective, where 39.2 ± 74.9 nm size can degrade 92.81% within 105 minutes that obeys pseudo-first-order kinetics (Malakootian *et al.*, 2020). Mascolo, G., et al 2007 reported that Methylene Red dye was photolytically degraded by TiO_2 Degussa P25 photocatalyst with optimum efficiency (Mascolo *et al.*, 2007).

Natural and synthetic dyes are the coloring organic substances widely used in food, clothes, paper, animated bodies, paints, and industry. Dyes are unstable compounds that degrade with time in the presence of acid, base, water, and sunlight. Some dyes are considered carcinogenic due to their toxic by-products, which are ultimately released into the waterbodies and deteriorate the quality of water (Ishak *et al.*, 2020; Lin *et al.*, 2023; Siva, 2007).

Materials and Methods

Chemicals

Titanium(IV) chloride dehydrate (99% pure, 260.5 g/mol, CAS No. 7646-78-8) was purchased from Merck, India. Sodium hydroxide (99% pure, CAS No. 1310-73-2, 40 g/mol, MQ200) was purchased from Merck India. Similarly, Polyethylene Glycol PEG ($HO(C_2H_4O)n7H$, Mol wt. = 100 g/L, H_2O at 20^oC, CAS No. 25322-68-3) was purchased from Merck, India. Methylene blue (CAS No. 61-73-4, Mol wt. 319.86 g/mol) was purchased from Merck, India. Ethanol (C_2H_5OH, >99% purity, Mol wt. = 46.06 g/mol, CAS No. 64-17-5) was purchased from Fusion Biotech India. The distilled water was prepared at the Nanotechnology Laboratory RECAST, TU, Kirtipur, Kathmandu.

Synthesis of TiO_2 NPs by Co-precipitation Method

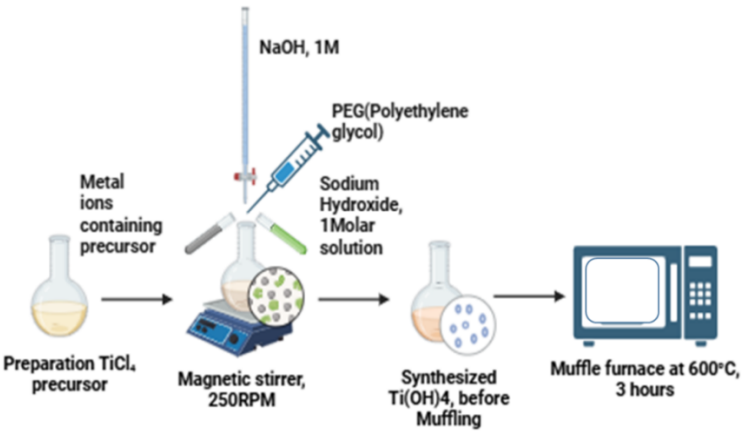

Fig. 1. Synthetic pathway for the synthesis of Titanium Oxide nanoparticle by Co-precipitation method.

Titanium chloride precursor was prepared by dissolving 18.967 gm of $TiCl_4$ salt in 1 liter of deionized distilled water to prepare a decimolar solution. The sodium hydroxide unit molar solution was prepared by dissolving 40 gm in 1 liter of water. When 100 ml of precursor was stirred at 25 ^oC at 250 RPM for 30 minutes, sodium hydroxide was added dropwise from the burette until the pH of the solution reached 6. A white mass of titanium hydroxide was obtained that was followed by adding polyethylene glycol (PEG) from the syringe as shown in Figure 1. The size of the particle was controlled to avoid the accumulation of particles into solid mass by PEG. When the stirring starts, titanium hydroxide is formed at room temperature, which is stored in a hot air oven at 60 ^oC for 24 hours for aging. The process was followed by muffling the solid at 600 ^oC for 3 hours, which gave a white crystalline powder particle of titanium oxide nanoparticle, which was stored in an airtight glass bottle. (Bagheri *et al.*, 2015; Chandoliya *et al.*, 2024; Matijevic, 1981; Wang *et al.*, 2022).

Characterization of Titanium Oxide Nanoparticles (TiO_2 NPs)

The TiO_2 NPs were characterized by UV-visible double-beam spectrophotometer (UV-1900i, Shimadzu, Japan). The Fourier Transfer Infra-red (FT-IR, IR Affinity-1s, Shimadzu, Japan) was analyzed to find the stretching and bending of TiO_2 NPs in a specific wavenumber region. Energy Dispersive X-ray (EDX-8000, Shimadzu, Japan) spectra were analyzed to identify elemental composition. The X-rd. spectra were analyzed by an X-ray Diffractometer (Bruker D2 Phaser, Massachusetts, USA) for the crystallographic texture, size of particles, and crystallinity of the sample.

Photocatalytic activity of TiO_2 Nanoparticle (TiO_2 NPs)

Titanium Oxide Nanoparticles is one of the best semiconducting catalysts, which is used for catalytic degradation of organic dyes, efficient organic synthesis, and semiconducting tuning of material properties. When solar radiation falls on the nanoparticles, the valence electron excites to

the conducting bands efficiently, leaving holes in the surface. The electron-hole pair formation mechanism produces a photoelectron that generates very powerful free radicals and superoxide, which initiates the photocatalytic degradation of dyes. In the present research, we have studied different kinetics and thermodynamic parameters for the illustration of photocatalytic degradation mechanisms. The solar radiation was supplied in August, having an average intensity of 5.76 $\pm$ 0.14 kWh in August 2024. The efficiency and kinetics were determined from the following equation.

$$-K_t = \ln\frac{C_t}{C_o} \quad \ldots\ldots\ldots 1$$

Where K_t is the rate of degradation of zero order kinetics, C_t is the final concentration of methylene blue and C_o is the initial concentration. The following relation determines the catalytic efficiency (Regmi *et al.*, 2015).

$$\text{Efficiency } (\%) = \frac{C_o - C_t}{C_o} \quad \ldots\ldots\ldots 2$$

Results and Discussion

UV-visible Spectra for Wavelength and Band Gap Calculation

The maximum wavelength absorption was found at 285 nm. Which is almost near the absorbance intensity of the reported value. Wavelength absorbance was determined from the 10 PPM TiO_2 NPs stock solution before the photocatalytic degradation. The band gap was calculated based on the intensity of the wavelength of the catalytic solution. The extrapolation of the plot gave the band gap of 3.25 eV, which is lower than the reported values due to the presence of insignificant concentrations of metallic impurities in the $TiCl_4$ salt (Akshay *et al.*, 2019; Glassford & Chelikowsky, 1992; Mo & Ching, 1995; Morikawa *et al.*, 2001; Reddy *et al.*, 2003; Reddy *et al.*, 2003; Umebayashi *et al.*, 2002).

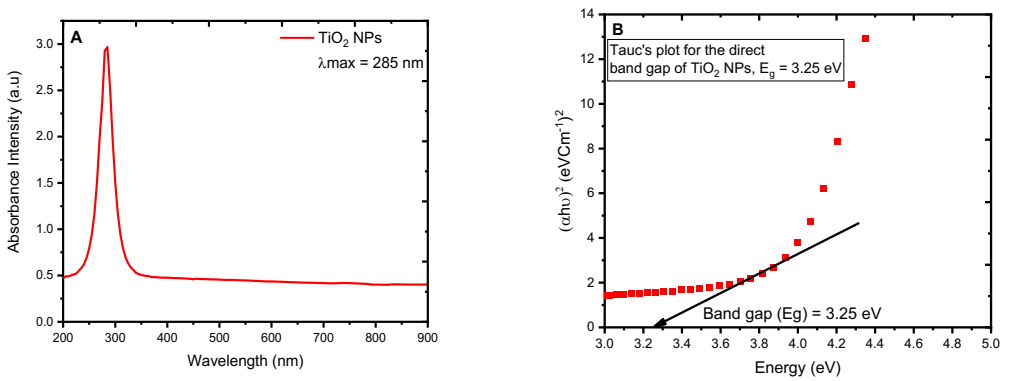

Fig. 2. Wavelength vs absorbance intensity for maximum of Titanium Oxide nanoparticles plot A) shows λ_{max} = 285 nm, and B) Tauc's plot for the direct band gap calculation of Titanium oxide nanoparticles.

FT-IT Spectra Analysis for TiO_2 NP

FT-IR analysis reveals that O-Ti-O strong stretching is obtained at 538.22 Cm^{-1}, confirming particle presence in the sample. The TiO_2 Nps also shows the water molecules due to moisture, which was found at 3457.70 Cm^{-1} stretching of the O-H bond. The plot depicts that very small C-H stretching at 2941.31 Cm^{-1} due to the presence of hydrocarbon, probably the trace concentration of alcohol in the sample. The plot also reveals that the nanoparticle also contains a Zirconium (Zr) bond with Oxygen (O) which is observed at 1653.56 Cm^{-1}, indicating the presence of a trace carbonyl group formed during synthesis. Similarly, the particle also shows a Niobium (Nb) and Oxygen (O) bond stretching at 978.53 Cm^{-1}. The sharp stretching of H-O-H is observed at 1116.94 Cm^{-1} (Chen *et al.*, 2012; Erdem *et al.*, 2001; Pena *et al.*, 2006; Zhang *et al.*, 2002).

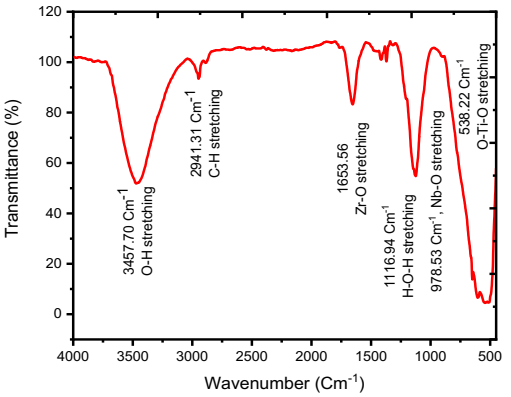

Fig. 3. FT-IR analysis for the TIO_2 NPs showing O-Ti-O stretching at different wavenumber regions.

EDX Spectra Analysis for TiO_2 NPs

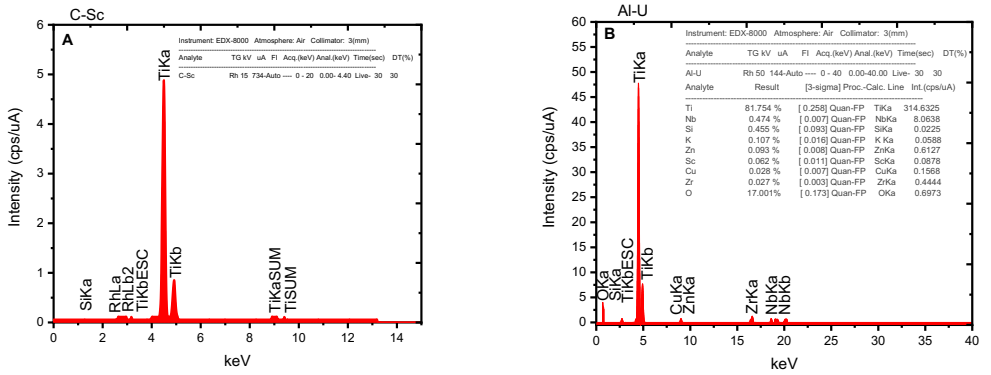

Fig. 4. EDX spectra of TiO_2 NPs A) showing the elemental composition of Titanium and Oxygen in C-Sc. B) EDX spectra of TiO_2 NPs showing high resolution of Al-U mode, showing the elemental composition of Titanium and Oxygen.

The EDX spectra are obtained in two different C-Sc and Al-U modes. The elemental compositions are distinctly observed in figures A and B. When intensity (cps/uA) vs. keV reveals the composition of different constituent elements in the particle, EDX spectra of TiO_2 NPs reveal that the synthesized particle contains 81.75% Titanium (Ti) in 4.514 keV, 17.001% Oxygen (O) in 0.601 keV. The additional peaks show that 0.474% Niobium (Nb) in 18.56 keV, 0.475% Silicon (Si) in 2.07 keV, 0.107% Potassium (K) in 0.058 keV, 0.093% Zinc (Zn) in 10 keV, 0.062% Scandium (Sc) in 0.087 keV, 0.028% Copper (Cu) in 0.156 keV, and % Zirconium (Zr) in 16.56 keV. The trace composition of the metals Nb, Si, K, Zn, Sc, Cu also decreases the band gap of the particle. Still, their trace composition < 1% does not show a significant effect in the photocatalytic degradation of methylene blue (Albayrak *et al.*, 2008; Atchudan *et al.*, 2017; Bahjat *et al.*, 2021; Irshad *et al.*, 2020; Kolen'ko *et al.*, 2006; Nkele *et al.*, 2020; Sundrarajan *et al.*, 2017; Windler *et al.*, 2012).

X-RD Crystallography Analysis of TiO_2 NPs

X-RD diffraction shows the distinct miller indices for the anatase geometry of TiO_2 NPs. The characteristic 110 peaks having $2\theta = 24.90^o$ with the highest intensity 5794.85 is obtained. Similarly the additional peak at 101 ($2\theta = 30.14$, Intensity 151.669), 101 ($2\theta = 30.14^o$, Intensity 151.669), 200 ($2\theta = 37.69^o$, Intensity 793.43), 210 ($2\theta = 47.57^o$, Intensity 1528.2965), 211 ($2\theta = 53.67^o$, Intensity 977.6457), 220 ($2\theta = 54.54^o$, Intensity 999.4340), 310 ($2\theta = 62.36^o$, Intensity 678.5512), 301 ($2\theta = 68.49^o$, Intensity 242.78438), 112 ($2\theta = 69.94^o$, Intensity 220.9960), 311 ($2\theta = 75.18^o$, Intensity 312.11092), 202 ($2\theta = 82.73^o$, Intensity 197.22693).

These peaks confirm the crystalline anatase geometry of TiO_2 nanoparticles. The peak analysis shows that TiO_2 NPs have (FWHA)β = 0.0087266 radians for 101 peak 2θ = 24.90°, λ = 0.154 nm (CuK_α), shape factor (K) = 0.9 (Gupta *et al.*, 2010; Pratheepa & Lawrence, 2017; Praveen *et al.*, 2014; Su *et al.*, 2004; Theivasanthi & Alagar, 2013).

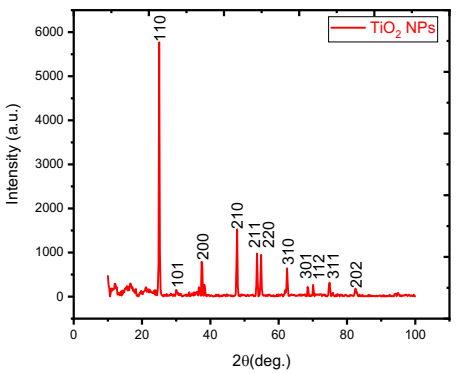

Fig. 5. X-RD crystallography showing the different Millar Indices of Anatage TiO_2 NPs.

According to Debye Scherer's equation, the following relations determine the diameter of the particle (Basak *et al.*, 2022; Bradley & Jay, 1932; Stokes & Wilson, 1942; Taylor & Sinclair, 1945).

$$D = \frac{K\lambda}{\beta Cos\theta} = \frac{0.9 \text{ x } 0.154}{0.0087266 \text{ x } Cos\ (12.45^{o})} \approx 16.27 \text{ nm}$$

Similarly, the crystallinity of TiO_2 NPs is calculated from the peak.

$$\text{Crystallinity } (\%) = \frac{\text{Total Crystalline Area}}{\text{Crystalline Area} + \text{Amorphous Area}} \text{ x } 100$$

$$= \frac{4167.095}{7290.81} \text{ x } 100 = 57.15\%$$

The X-RD spectra analysis reveals that the synthesized nanoparticle has a size of 16.27 nm and 57.15% crystallinity. The lattice parameter shows that the length of each respective side is a = 3.73000, b = 3.73000, and c = 9.37000, with their inter-axial angles α = 90°, β = 90°, and γ = 90° having a unit cell volume of 130.363873 Å^3. A perfect anatase structure of TiO_2 contains 63 atoms, 78 bonds, and 13 polyhedra, as shown in Figure 6 (Gražulis *et al.*, 2012; Momma & Izumi, 2008).

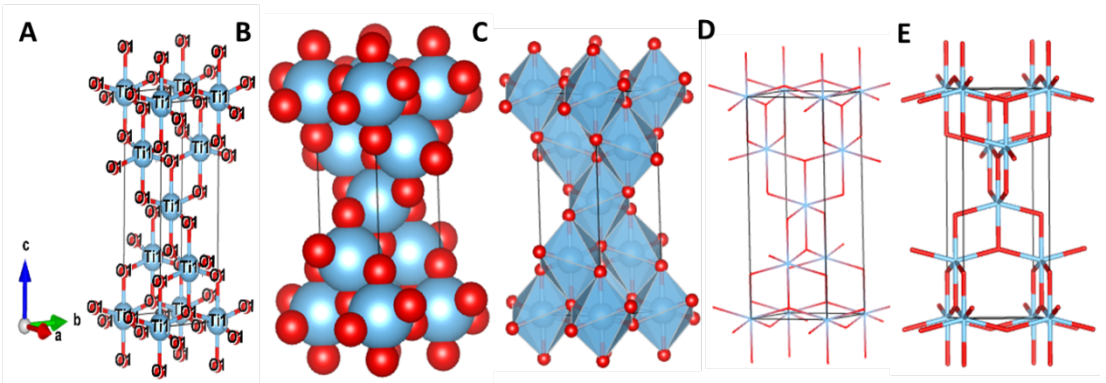

Fig. 6. Anatage 3D structure of TiO_2 NPs showing A) Ball and stick, B) space-filling, C) polyhedral, D & E) wireframe representation. 3D structures are generated from VESTA(Visualizing Crystal Structures) based on Crystallography Open databases.

Solar Intensity for Photocatalytic Degradation

The semiconducting nanoparticle Titanium oxide absorbs solar light at about the average solar intensity of 5.74±0.14 kWh. When a nanoparticle absorbs light, the electron from the valence band excites to the conducting bands; as a result, an electron-hole pair is formed. Electrons generate powerful superoxide radicals and holes form hydroxide free radicals. Both active radicals degrade methylene blue dyes into simple chemical substances. Solar intensity significantly affects the formation of radicals and enhances the photocatalytic degradation process (Chowdhury *et al.*, 2012; Neppolian *et al.*, 2002; Stylidi *et al.*, 2003). The present research work was conducted in August, and the distribution of solar radiation is shown in Figure 7.

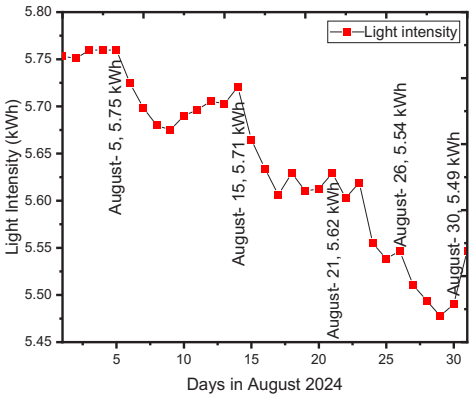

Fig. 7. Solar radiation intensity in August 2024.

The solar radiation absorbed by TiO_2 NPs excites the electron from the surface of nanoparticles, which is followed by the formation of free radicals. Thus, the formed free radical reduces methylene blue, and simultaneously recombination of the electron-hole takes place, which may reduce the degradation process. The following illustrative diagram explains the mineralization of dyes into a safer and simpler chemical compound (Muruganandham & Swaminathan, 2004; Sakthivel *et al.*, 2003).

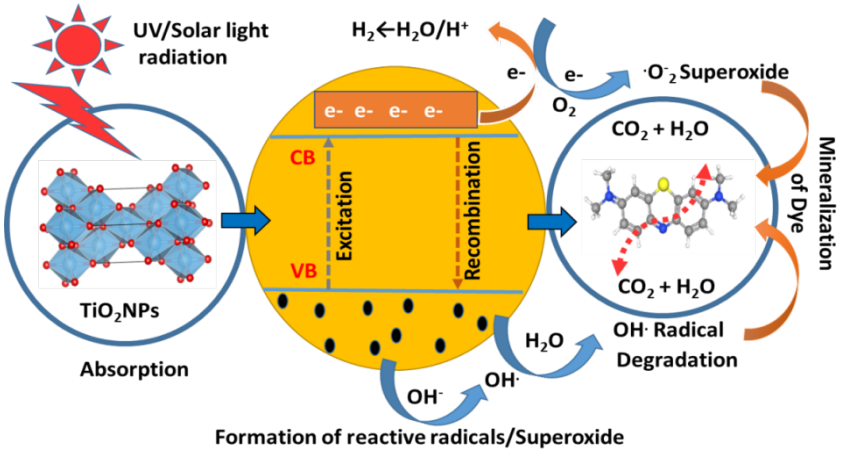

Fig. 8. Photocatalytic degradation mechanism showing absorption, excitation, formation of electron-hole pair, recombination, and degradation of dyes.

Photocatalytic Degradation of Methylene Blue

The experiment was conducted by the preparation of respective 10 ppm stock solution of methylene blue. The experiment was carried out by adding 100 ml solution in a transparent borosilicate glass and adding 10 mg TiO_2 NPs at a solar intensity of 5.74 ± 0.14 kWh. Gradually, the blue-color dye solution appears into a faint blue

color. The process continues until the complete degradation occurs. The successive experiment was conducted with persistent light intensity. The initial reading was taken in the dark medium, which was continuously recorded in light. The photocatalytic degradation was completed in 90 minutes, but the degradation was incomplete and continued at a slow rate in the dark medium. The degradation was recorded until 130 minutes, and infinite degradation was calculated, which was found insignificant as compared to the solar light degradation. After the completion of degradation, the entire solution was centrifuged at 5500 RPM, the nanoparticle was settled down at the bottom of the tube that was used again for three successive cycles. The catalytic nature and strength of TiO_2 remain intact. The maximum wavelength absorption intensity for methylene blue was recorded at 665 nm (Kuo & Ho, 2001; Tayade *et al.*, 2009; Wang *et al.*, 2010; Xiao *et al.*, 2008).

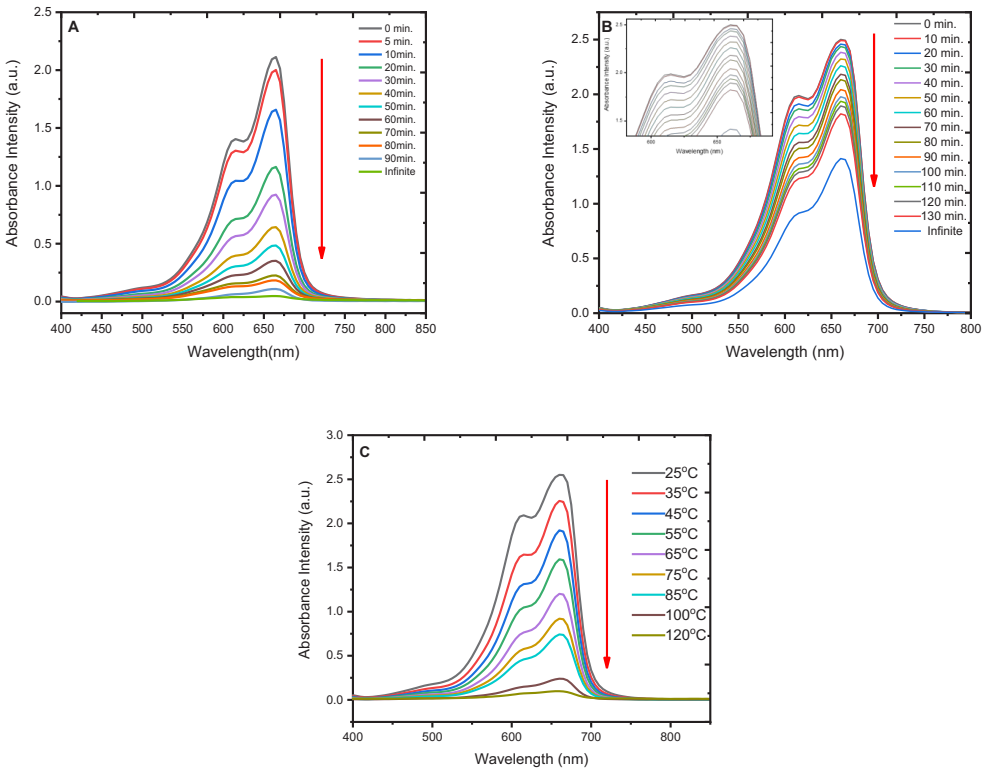

Fig. 9. Photocatalytic degradation of methylene blue in A) Solar light B) Dark C) Solar light and heating. The figure shows the maximum time required for the degradation of methylene blue in light was 90 minutes, in the dark medium the degradation was in complete and prolonged up to 130 minutes and in both light and heat, the degradation was completed in 80 minutes and 120 °C.

The photocatalytic degradation for methylene blue was more efficient when heating the solution over a magnetic stirrer. The result reveals that 50% of the methylene blue solution was degraded within 40 minutes. The heating enhances the degradation more profoundly than in light and dark mediums. The result shows complete degradation was achieved in 70 minutes at 120 ^{o}C.

The photocatalytic degradation mechanism starts with the absorption of solar light. The absorbed light excites the electrons from titanium oxide nanoparticles. Hence, the excitation of electrons takes place from the valence band to the conducting, and that forms an electron-hole pair. The formation of these pairs generates hydroxide free radicals and superoxide. While occurring such a phenomenon, the recombination of the electron-hole pair reduces the catalytic activity, probably it is due to the low intensity of solar radiation on the nanoparticles. The mineralization of methylene blue into CO_2 and H_2O confirms its efficient degradation, which can be expressed by the following reaction mechanism (Hoffmann *et al.*, 1995; Mekonnen *et al.*, 2021). The photocatalytic degradation mechanism can be explained in the following chemical equations.

TiO_2 NPs + $h\vartheta \rightarrow$ $TiO_2 (e^-)_{CB}$ + $TiO_2 (H+)_{VB}$ 1

$TiO_2 (Hole+)_{VB} + H_2O \rightarrow H^+ + OH^-$ (ions) 2

$TiO_2 (Hole+)_{VB} + OH^- \rightarrow OH^{\cdot}$ (Radicals) 3

$4OH^-$(Solution) $\rightarrow 2H_2O + O_2$ 4

$TiO_2 (e-)_{CB} + O_2 \rightarrow {\cdot}O_2^-$ (Superoxide) 5

Methylene Blue + OH^- (Radical) $\rightarrow CO_2 + H_2O$ 6

Methylene Blue + $O_2^- \rightarrow CO_2 + H_2O$ 7

Kinetics of Photocatalytic Degradation

The plot of C/C_o vs. time and $\ln(C/C_o)$ vs. time is plotted for the analysis of kinetic parameters through statistical tools. The catalytic degradation of methylene blue in light, dark, and heat strictly obeys pseudo-first-order kinetics. The statistical analysis reveals that photocatalytic degradation has a slope of -0.00321$\pm$0.000366, and an intercept obtained is 0.06274$\pm$0.03012. The plot shows Pearson's *r* -0.92479 and the adjusted correlation coefficient (R^2) is 0.844. The degradation of dye in the dark also obeys pseudo-first-order kinetics, having a slope of -0.03317$\pm$0.0019 with an intercept of 0.35468$\pm$0.12358. The plot shows that the Pearson's *r* obtained is -0.98394 and the adjusted correlation coefficient (R^2) is 0.964. The photocatalytic degradation of methylene blue in light by increasing temperature flows pseudo-first-order kinetics having slope -0.03563$\pm$0.00482 with an intercept of -1.29809$\pm$0.35579. The Pearson's *r* obtained from the plot is -0.941, and the adjusted correlation coefficient (R^2) is 0.869 (Konstantinou & Albanis, 2004; Mahmoodi *et al.*, 2006; Sauer *et al.*, 2002).

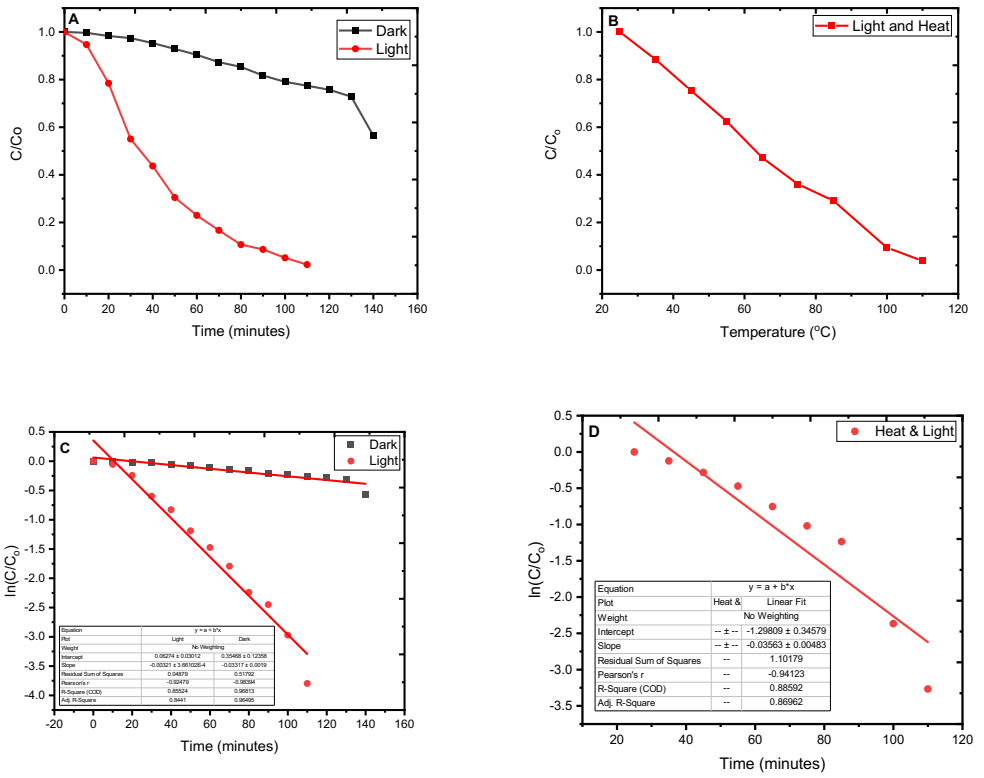

Fig. 10. Kinetics for the photocatalytic degradation showing A and B) C/C_o vs time for light and dark and C) $\ln(C/C_o)$ vs times (minutes) showing linear plot for the degradation, D) shows the linear plot for the photocatalytic degradation in heat and light.

Catalytic Efficiency of TiO_2 NPs

The catalytic efficiency of methylene blue in light is found stronger than in dark. The result reveals that 98% methylene blue degrades within 110 minutes but in dark, the efficiency is 48% and still incomplete and slowly prolongs up to 140 minutes. When temperature increases gradually, the degradation becomes more feasible and completed within 70 minutes having an efficiency of 98% (Fathinia *et al.*, 2010; Kitture *et al.*, 2011).

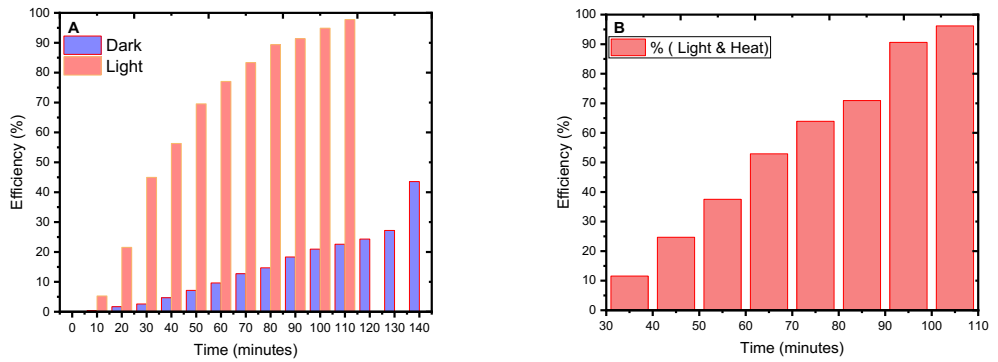

Fig. 11. A plot of efficiency (%) vs time for the degradation of methylene blue by TiO_2 NPs. Figure A) shows the catalytic efficiency 98% achieved in 110 minutes and 48% efficiency achieved in 140 minutes in the dark Figure B) shows a similar result having a catalytic efficiency of 98% in light-enhancing temperature only in 70 minutes.

Conclusion

Titanium oxide nanoparticles are very reactive catalysts. Their potential application has been applied for the photocatalytic degradation of dyes. Methylene blue is a common dye used in laboratory and textile industries, having a strong factor of toxicity and carcinogen in human health. In the present work, we have synthesized titanium oxide nanoparticles by the co-precipitation method through a controlled pH pathway. The synthesized TiO_2 NPs are characterized by UV-Spectrophotometer, where we obtained a 285 nm wavelength for the particle. The band gap of 3.25 eV is calculated by the extrapolation of Tauc's plot. The TiO_2 NPs are characterized by FT-IT that shows O-Ti-O strong stretching at 538.22 Cm^{-1}. Furthermore, EDX spectra of TiO_2 NPs reveal that the synthesized particle contains 81.75% Titanium (Ti) in 4.514 keV and 17.001% Oxygen(O) in 0.601 keV. The size of TiO_2 NPs is determined by solving Debye Scherer's equation; the average diameter of the particle is found 16.27 ± 12.80nm with 57.15% crystallinity. The photocatalytic degradation is carried out in the solar intensity of 5.76 ± 0.14 kWh for methylene blue, which is recorded at 665 nm in UV-visible spectrophotometer. It is found that methylene blue is completely degraded in solar light within 110 minutes with 98% catalytic efficiency, but the dark medium degradation is not completed until 140 minutes and is limited to its 48% efficiency. The temperature-enhancing degradation in solar light is completed in 70 minutes with 98% efficiency. The catalytic efficiency of TiO_2 NPs in light is superior to that in the dark, which explores its potential application as a photocatalyst.

Declaration

The authors of this article declare no conflict of interest.

References

Akpan, U. G., & Hameed, B. H. (2009). Parameters affecting the photocatalytic degradation of dyes using TiO2-based photocatalysts: a review. *Journal of Hazardous Materials*, *170*(2–3), 520–529.

Akshay, V. R., Arun, B., Mandal, G., & Vasundhara, M. (2019). Visible range optical absorption, Urbach energy estimation and paramagnetic response in Cr-doped TiO 2 nanocrystals derived by a sol–gel method. *Physical Chemistry Chemical Physics*, *21*(24), 12991–13004.

Albayrak, O., El-Atwani, O., & Altintas, S. (2008). Hydroxyapatite coating on titanium substrate by electrophoretic deposition method: effects of titanium dioxide inner layer on adhesion strength and hydroxyapatite decomposition. *Surface and Coatings Technology*, *202*(11), 2482–2487.

Atchudan, R., Edison, T. N. J. I., Perumal, S., Karthikeyan, D., & Lee, Y. R. (2017). Effective photocatalytic degradation of anthropogenic dyes using graphene oxide grafting titanium dioxide nanoparticles under UV-light irradiation. *Journal of Photochemistry and Photobiology A: Chemistry*, *333*, 92–104.

Bagheri, S., Mohd Hir, Z. A., Yousefi, A. T., & Abdul Hamid, S. B. (2015). Progress on mesoporous titanium dioxide: Synthesis, modification and applications. *Microporous and Mesoporous Materials*, *218*, 206–222. https://doi.org/https://doi.org/10.1016/j.micromeso.2015.05.028

Bahjat, H. H., Ismail, R. A., Sulaiman, G. M., & Jabir, M. S. (2021). Magnetic field-assisted laser ablation of titanium dioxide nanoparticles in water for anti-bacterial applications. *Journal of Inorganic and Organometallic Polymers and Materials*, *31*(9), 3649–3656.

Basak, M., Rahman, M. L., Ahmed, M. F., Biswas, B., & Sharmin, N. (2022). The use of X-ray diffraction peak profile analysis to determine the structural parameters of cobalt ferrite nanoparticles using Debye-Scherrer, Williamson-Hall, Halder-Wagner and Size-strain plot: Different precipitating agent approach. *Journal of Alloys and Compounds*, *895*, 162694.

Bradley, A. J., & Jay, A. H. (1932). A method for deducing accurate values of the lattice spacing from X-ray powder photographs taken by the Debye-Scherrer method. *Proceedings of the Physical Society*, *44*(5), 563.

Chandoliya, R., Sharma, S., Sharma, V., Joshi, R., & Sivanesan, I. (2024). Titanium Dioxide Nanoparticle: A Comprehensive Review on Synthesis, Applications and Toxicity. *Plants*, *13*(21). https://doi.org/10.3390/plants13212964

Chen, H., Nanayakkara, C. E., & Grassian, V. H. (2012). Titanium dioxide photocatalysis in atmospheric chemistry. *Chemical Reviews*, *112*(11), 5919–5948.

Chin, S., Park, E., Kim, M., & Jurng, J. (2010). Photocatalytic degradation of methylene blue with TiO2 nanoparticles prepared by a thermal decomposition process. *Powder Technology*, *201*(2), 171–176.

Chowdhury, P., Moreira, J., Gomaa, H., & Ray, A. K. (2012). Visible-solar-light-driven photocatalytic degradation of phenol with dye-sensitized TiO2: parametric and kinetic study. *Industrial & Engineering Chemistry Research*, *51*(12), 4523–4532.

Erdem, B., Hunsicker, R. A., Simmons, G. W., Sudol, E. D., Dimonie, V. L., & El-Aasser, M. S. (2001). XPS and FTIR surface characterization of TiO2 particles used in polymer encapsulation. *Langmuir*, *17*(9), 2664–2669.

Fathinia, M., Khataee, A. R., Zarei, M., & Aber, S.

(2010). Comparative photocatalytic degradation of two dyes on immobilized TiO2 nanoparticles: effect of dye molecular structure and response surface approach. *Journal of Molecular Catalysis A: Chemical*, *333*(1–2), 73–84.

Glassford, K. M., & Chelikowsky, J. R. (1992). Structural and electronic properties of titanium dioxide. *Physical Review B*, *46*(3), 1284.

Gražulis, S., Daškevič, A., Merkys, A., Chateigner, D., Lutterotti, L., Quiros, M., Serebryanaya, N. R., Moeck, P., Downs, R. T., & Le Bail, A. (2012). Crystallography Open Database (COD): an open-access collection of crystal structures and platform for world-wide collaboration. *Nucleic Acids Research*, *40*(D1), D420–D427.

Gupta, S. K., Desai, R., Jha, P. K., Sahoo, S., & Kirin, D. (2010). Titanium dioxide synthesized using titanium chloride: size effect study using Raman spectroscopy and photoluminescence. *Journal of Raman Spectroscopy: An International Journal for Original Work in All Aspects of Raman Spectroscopy, Including Higher Order Processes, and Also Brillouin and Rayleigh Scattering*, *41*(3), 350–355.

Hoffmann, M. R., Martin, S. T., Choi, W., & Bahnemann, D. W. (1995). Environmental applications of semiconductor photocatalysis. *Chemical Reviews*, *95*(1), 69–96.

Irshad, M. A., Nawaz, R., ur Rehman, M. Z., Imran, M., Ahmad, J., Ahmad, S., Inam, A., Razzaq, A., Rizwan, M., & Ali, S. (2020). Synthesis and characterization of titanium dioxide nanoparticles by chemical and green methods and their antifungal activities against wheat rust. *Chemosphere*, *258*, 127352.

Ishak, S. A., Murshed, M. F., Md Akil, H., Ismail, N., Md Rasib, S. Z., & Al-Gheethi, A. A. S. (2020). The application of modified natural polymers in toxicant dye compounds wastewater: A review. *Water*, *12*(7), 2032.

Jallouli, N., Elghniji, K., Trabelsi, H., & Ksibi, M. (2017). Photocatalytic degradation of paracetamol on TiO2 nanoparticles and TiO2/cellulosic fiber under UV and sunlight irradiation. *Arabian Journal of Chemistry*, *10*, S3640–S3645.

Jamkhande, P. G., Ghule, N. W., Bamer, A. H., & Kalaskar, M. G. (2019). Metal nanoparticles synthesis: An overview on methods of preparation, advantages and disadvantages, and applications. *Journal of Drug Delivery Science and Technology*, *53*, 101174.

Kansal, S. K., Sood, S., Umar, A., & Mehta, S. K. (2013). Photocatalytic degradation of Eriochrome Black T dye using well-crystalline anatase TiO2 nanoparticles. *Journal of Alloys and Compounds*, *581*, 392–397.

Kitture, R., Koppikar, S. J., Kaul-Ghanekar, R., & Kale, S. N. (2011). Catalyst efficiency, photostability and reusability study of ZnO nanoparticles in visible light for dye degradation. *Journal of Physics and Chemistry of Solids*, *72*(1), 60–66.

Kolen'ko, Y. V, Kovnir, K. A., Gavrilov, A. I., Garshev, A. V, Frantti, J., Lebedev, O. I., Churagulov, B. R., Van Tendeloo, G., & Yoshimura, M. (2006). Hydrothermal synthesis and characterization of nanorods of various titanates and titanium dioxide. *The Journal of Physical Chemistry B*, *110*(9), 4030–4038.

Konstantinou, I. K., & Albanis, T. A. (2004). TiO2-

assisted photocatalytic degradation of azo dyes in aqueous solution: kinetic and mechanistic investigations: a review. *Applied Catalysis B: Environmental*, *49*(1), 1–14.

Kumar, A., Choudhary, P., Kumar, A., Camargo, P. H. C., & Krishnan, V. (2022). Recent advances in plasmonic photocatalysis based on TiO2 and noble metal nanoparticles for energy conversion, environmental remediation, and organic synthesis. *Small*, *18*(1), 2101638.

Kuo, W. S., & Ho, P. H. (2001). Solar photocatalytic decolorization of methylene blue in water. *Chemosphere*, *45*(1), 77–83.

Lin, J., Ye, W., Xie, M., Seo, D. H., Luo, J., Wan, Y., & Van der Bruggen, B. (2023). Environmental impacts and remediation of dye-containing wastewater. *Nature Reviews Earth & Environment*, *4*(11), 785–803.

Mahmoodi, N. M., Arami, M., Limaee, N. Y., & Tabrizi, N. S. (2006). Kinetics of heterogeneous photocatalytic degradation of reactive dyes in an immobilized TiO2 photocatalytic reactor. *Journal of Colloid and Interface Science*, *295*(1), 159–164.

Malakootian, M., Nasiri, A., & Amiri Gharaghani, M. (2020). Photocatalytic degradation of ciprofloxacin antibiotic by TiO2 nanoparticles immobilized on a glass plate. *Chemical Engineering Communications*, *207*(1), 56–72.

Mascolo, G., Comparelli, R., Curri, M. L., Lovecchio, G., Lopez, A., & Agostiano, A. (2007). Photocatalytic degradation of methyl red by TiO2: Comparison of the efficiency of immobilized nanoparticles versus conventional suspended catalyst. *Journal of Hazardous Materials*, *142*(1–2), 130–137.

Matijevic, E. (1981). Monodispersed metal (hydrous) oxides-a fascinating field of colloid science. *Accounts of Chemical Research*, *14*(1), 22–29.

Mekonnen, T. B., Mengesha, A. T., & Dube, H. H. (2021). Photocatalytic Degradation of Organic Pollutants: The Case of Conductive Polymer Supported Titanium Dioxide (TiO2) Nanoparticles: A Review. *Nanoscience and Nanometrology*, *7*(1), 1–13. https://doi.org/10.11648/j.nsnm.20210701.11

Mo, S.-D., & Ching, W. Y. (1995). Electronic and optical properties of three phases of titanium dioxide: Rutile, anatase, and brookite. *Physical Review B*, *51*(19), 13023.

Momma, K., & Izumi, F. (2008). VESTA: a three-dimensional visualization system for electronic and structural analysis. *Journal of Applied Crystallography*, *41*(3), 653–658.

Morikawa, T., Asahi, R., Ohwaki, T., Aoki, K., & Taga, Y. (2001). Band-gap narrowing of titanium dioxide by nitrogen doping. *Japanese Journal of Applied Physics*, *40*(6A), L561.

Muruganandham, M., & Swaminathan, M. (2004). Solar photocatalytic degradation of a reactive azo dye in TiO2-suspension. *Solar Energy Materials and Solar Cells*, *81*(4), 439–457.

Neppolian, B., Choi, H. C., Sakthivel, S., Arabindoo, B., & Murugesan, V. (2002). Solar/UV-induced photocatalytic degradation of three commercial textile dyes. *Journal of Hazardous Materials*, *89*(2–3), 303–317.

Nkele, A. C., Chime, U. K., Asogwa, L., Nwanya, A. C., Nwankwo, U., Ukoba, K., Jen, T. C.,

Maaza, M., & Ezema, F. I. (2020). A study on titanium dioxide nanoparticles synthesized from titanium isopropoxide under SILAR-induced gel method: Transition from anatase to rutile structure. *Inorganic Chemistry Communications*, *112*, 107705.

Nyamukamba, P., Okoh, O., Mungondori, H., Taziwa, R., & Zinya, S. (2018). Synthetic methods for titanium dioxide nanoparticles: a review. *Titanium Dioxide-Material for a Sustainable Environment*, *8*, 151–175.

Pena, M., Meng, X., Korfiatis, G. P., & Jing, C. (2006). Adsorption mechanism of arsenic on nanocrystalline titanium dioxide. *Environmental Science & Technology*, *40*(4), 1257–1262.

Pratheepa, M. I., & Lawrence, M. (2017). X-ray diffraction analyses of titanium dioxide nanoparticles. *Int J Sci Res Sci Technol*, *3*(11), 83–88.

Praveen, P., Viruthagiri, G., Mugundan, S., & Shanmugam, N. (2014). Structural, optical and morphological analyses of pristine titanium di-oxide nanoparticles–Synthesized via sol–gel route. *Spectrochimica Acta Part A: Molecular and Biomolecular Spectroscopy*, *117*, 622–629.

Rane, A. V., Kanny, K., Abitha, V. K., & Thomas, S. (2018). Methods for synthesis of nanoparticles and fabrication of nanocomposites. In *Synthesis of inorganic nanomaterials* (pp. 121–139). Elsevier.

Reddy, K. M., Manorama, S. V, & Reddy, A. R. (2003). Bandgap studies on anatase titanium dioxide nanoparticles. *Materials Chemistry and Physics*, *78*(1), 239–245.

Reddy, K., Sunkara, M., & Reddy, A. (2003). Bandgap Studies on Anatase Titanium Dioxide Nanoparticles. *Materials Chemistry and Physics*, *78*, 239–245. https://doi.org/10.1016/S0254-0584(02)00343-7

Regmi, S., Ghimire, K. N., Pokhrel, M. R., & Khadka, D. B. (2015). Adsorptive removal and recovery of aluminium (III), iron (II), and chromium (VI) onto a low cost functionalized phragmities karka waste. *Journal of Institute of Science and Technology*, *20*(2), 145–152.

Reza, K. M., Kurny, A. S. W., & Gulshan, F. (2017). Parameters affecting the photocatalytic degradation of dyes using TiO 2: a review. *Applied Water Science*, *7*, 1569–1578.

Sakthivel, S., Neppolian, B., Shankar, M. V, Arabindoo, B., Palanichamy, M., & Murugesan, V. (2003). Solar photocatalytic degradation of azo dye: comparison of photocatalytic efficiency of ZnO and TiO2. *Solar Energy Materials and Solar Cells*, *77*(1), 65–82.

Sauer, T., Neto, G. C., Jose, H. J., & Moreira, R. (2002). Kinetics of photocatalytic degradation of reactive dyes in a TiO2 slurry reactor. *Journal of Photochemistry and Photobiology A: Chemistry*, *149*(1–3), 147–154.

Shaoqing, Y., Jun, H., & Jianlong, W. (2010). Radiation-induced catalytic degradation of p-nitrophenol (PNP) in the presence of TiO2 nanoparticles. *Radiation Physics and Chemistry*, *79*(10), 1039–1046.

Siva, R. (2007). Status of natural dyes and dye-yielding plants in India. *Current Science*, 916–925.

Stokes, A. R., & Wilson, A. J. C. (1942). A method of calculating the integral breadths of Debye-Scherrer lines. *Mathematical Proceedings of the Cambridge*

Philosophical Society, *38*(3), 313–322.

Stylidi, M., Kondarides, D. I., & Verykios, X. E. (2003). Pathways of solar light-induced photocatalytic degradation of azo dyes in aqueous TiO2 suspensions. *Applied Catalysis B: Environmental*, *40*(4), 271–286.

Su, C., Hong, B.-Y., & Tseng, C.-M. (2004). Sol–gel preparation and photocatalysis of titanium dioxide. *Catalysis Today*, *96*(3), 119–126.

Sundrarajan, M., Bama, K., Bhavani, M., Jegatheeswaran, S., Ambika, S., Sangili, A., Nithya, P., & Sumathi, R. (2017). Obtaining titanium dioxide nanoparticles with spherical shape and antimicrobial properties using M. citrifolia leaves extract by hydrothermal method. *Journal of Photochemistry and Photobiology B: Biology*, *171*, 117–124.

Tayade, R. J., Natarajan, T. S., & Bajaj, H. C. (2009). Photocatalytic degradation of methylene blue dye using ultraviolet light emitting diodes. *Industrial & Engineering Chemistry Research*, *48*(23), 10262–10267.

Taylor, A., & Sinclair, H. (1945). On the determination of lattice parameters by the Debye-Scherrer method. *Proceedings of the Physical Society*, *57*(2), 126.

Theivasanthi, T., & Alagar, M. (2013). Titanium dioxide (TiO2) nanoparticles XRD analyses: an insight. *ArXiv Preprint ArXiv:1307.1091*.

Umebayashi, T., Yamaki, T., Itoh, H., & Asai, K. (2002). Band gap narrowing of titanium dioxide by sulfur doping. *Applied Physics Letters*, *81*(3), 454–456.

Valencia, S., Marín, J. M., & Restrepo, G. (2010). Study of the bandgap of synthesized titanium dioxide nanoparticules using the sol-gel method and a hydrothermal treatment. *Open Materials Science Journal*, *4*(1), 9–14.

Wang, F., Min, S., Han, Y., & Feng, L. (2010). Visible-light-induced photocatalytic degradation of methylene blue with polyaniline-sensitized TiO2 composite photocatalysts. *Superlattices and Microstructures*, *48*(2), 170–180.

Wang, J., Wang, Z., Wang, W., Wang, Y., Hu, X., Liu, J., Gong, X., Miao, W., Ding, L., Li, X., & Tang, J. (2022). Synthesis{,} modification and application of titanium dioxide nanoparticles: a review. *Nanoscale*, *14*(18), 6709–6734. https://doi.org/10.1039/D1NR08349J

Windler, L., Lorenz, C., von Goetz, N., Hungerbuhler, K., Amberg, M., Heuberger, M., & Nowack, B. (2012). Release of titanium dioxide from textiles during washing. *Environmental Science & Technology*, *46*(15), 8181–8188.

Xiao, Q., Zhang, J., Xiao, C., Si, Z., & Tan, X. (2008). Solar photocatalytic degradation of methylene blue in carbon-doped TiO2 nanoparticles suspension. *Solar Energy*, *82*(8), 706–713.

Zhang, J.-Y., Boyd, I. W., O'sullivan, B. J., Hurley, P. K., Kelly, P. V, & Senateur, J.-P. (2002). Nanocrystalline TiO2 films studied by optical, XRD and FTIR spectroscopy. *Journal of Non-Crystalline Solids*, *303*(1), 134–138.